

Steric Protected and Illumination-Activated Tumor Targeting Accessory for Endowing Drug-Delivery Systems with Tumor Selectivity

Zhefan Yuan, Dan Zhao, Xiaoqing Yi, Renxi Zhuo, and Feng Li*

Here, an ABA-typed polymer, octadecyl-polyethylene glycol (biotin)-(o-nitrobenzyl)-octadecyl ester (CPB-p-C) with an o-nitrobenzyl group inserted between polyethylene glycol (PEG) and octadecyl ester is synthesized as an illumination-activated tumor targeting accessory for micelle-based drug carriers. The functional accessory can form a flower-like structure with folded PEG segments in aqueous solution to hide targeting biotin ligands in the core of the mixed micelle. Thus the specific binding between biotin and avidin can be suppressed by the steric hindrance of PEG shell. Upon illumination, the flower-like structure of CPB-p-C is destroyed due to the cleavage of the o-nitrobenzyl group and the biotin moieties are exposed on the surface of the micelle through the stretching process of PEG segments, generating ligand-receptor-mediated targeted delivery. By confocal laser scanning microscopy and flow cytometry, the illumination-activated, tumor-targeting delivery is studied. The influence of the amount of functional accessory in the mixed micelle on the targeting property is investigated and the optimal amount of CPB-p-C to achieve less side effects and better illumination activated tumor targeting activity is identified. The observed properties of CPB-p-C qualify it as a promising functional accessory to endow traditional drug-delivery systems with tumor selectivity.

develop tumor-targeting drug carriers anchored with targeting ligands, such as antibodies,^[1] vitamins,^[2] peptides^[3] and aptamers.^[4] These targeting molecules are capable of binding specific cell membrane receptors and benefit the drug carriers across cell barriers. Although direct anchoring targeting ligands on the surface of drug carriers could significantly enhance the drug accumulation in tumor cells status is more complicated and delivery systems face severe challenges, such as aggregation, rapid clearance and immunogenicity in physiological environment, before arriving at pathological tissues.^[5] The targeting ligands possibly not only fail to accomplish their missions but also become burdens due to the specific or nonspecific contact. In our opinion, ideal target-mediated delivery systems should have such properties as follows: the targeting ligands of drug carriers should be protected or their targeting functions should be shut down during the transporting process in systematic circulation, and then be activated at pathological sites.

1. Introduction

Chemotherapy, as an important treatment modality, has been widely used in cancer therapy along with radiotherapy and surgery. However, systemic administration of anti-tumor drugs usually leads to undesirable biodistribution and severe side effects. A promising approach to solve this problem is to

In other words, the delivery systems should have 'targeting protection and stimuli activation' properties. In previous studies on intelligent drug carriers,^[6–9] charge-conversion polymers attracted intensive research interest.^[6,10] Amine-rich polymers were reacted with some derivatives of maleic anhydride to form serum-stable anionic vehicles. When these vehicles located in slightly acidic environment of tumor tissues, the surface charge turned from negative to positive, resulting in an enhanced intracellular uptake *via* electrostatic interaction. Different from direct chemical modification, another approach is to physically block the contact opportunities between targeting ligands and receptors. Zhang's group has anchored a targeting drug carrier with acid-cleavable polyethylene glycol (PEG) shells to inactivate the targeting functions.^[11] Due to the detachment of PEG shells in acidic environment of tumor tissue, the exposed targeting ligands could facilitate cellular uptake. It is worth noting that these strategies all focused on the specific pH value in tumor tissues, which is slightly acidic ($6.8 < \text{pH} < 7.4$) in comparison with normal tissues. Since the operable pH scale is relatively narrow, it is hard to keep a balance between pH sensitivity and physiological stability, which limits their potential

Dr. Z. Yuan, D. Zhao, X. Yi, Prof. R. Zhuo, Prof. F. Li
Key Laboratory of Biomedical Polymers
of Ministry of Education
College of Chemistry and Molecular Science
Wuhan University
Wuhan, 430072, China
E-mail: lfsj2004@hotmail.com

Dr. Z. Yuan
State Key Laboratory of Chemical Engineering
Department of Chemical and Biological Engineering
Zhejiang University
Hangzhou, 310027, China



DOI: 10.1002/adfm.201301309

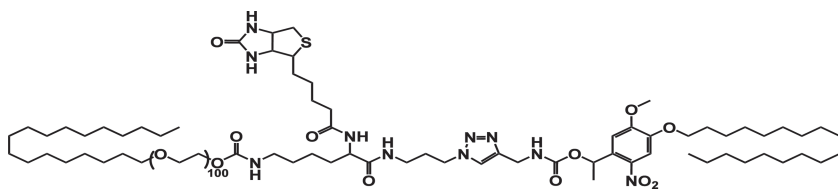


Figure 1. The structure of CPB-p-C.

applications.^[12] Therefore, there is an urgent need for additional breakthrough of tumor-specific targeting drug carriers.

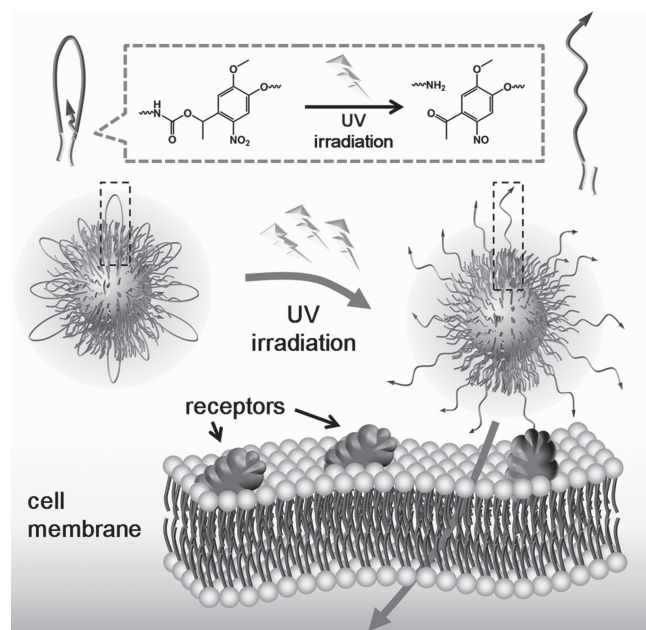
Light, different from tumor extracellular pH gradient, is a controllable external stimulus. Photochemical reaction and light-induced structural transformation can be completed within seconds or minutes by adjusting the parameters of external light source such as wavelength and intensity.^[13–15] Recently, Kohane's group reported an example of photo-targeted nanoparticles.^[16] This intelligent system was based on the photocaging method.^[17] The targeting peptide YIGSR on nanoparticles was firstly modified with 4,5-dimethoxy-2-nitrobenzyl (DMNB) group to inactivate its targeting function. Then DMNB was removed by UV-irradiation, leading to selective uptake of nanoparticles at illuminated sites. Similar strategies were also used to cage folic acid and the minimum sequence of cell penetrating peptide (RRMKWKK) by Yeh's^[18] and Ashkqenasy's^[19] groups, respectively. However, this photocaging method needs to cage every targeting ligand with more than one photo-cleavable moiety for effective inactivation, which may be helpless for those targeting ligands without (such as biotin) reaction site or with many reaction sites (such as long chain cell penetrating peptides). Furthermore, the caged ligands are still on the carrier surface and have to face complicated physiological environment to undergo unexpected changes.

Recently, Bae's group has reported a new approach to inactivate and activate the targeting function.^[20,21] In their studies, pLLA-*b*-PEG-*b*-polyHis-ligand tri-block polymers were prepared. The targeting ligands were shielded by folded PEG chains due to the hydrophobicity of polyHis block in physiological pH value. When the drug carrier exposed to weak acidic environment, the ligands were pushed to the micellar surface by the protonated polyHis block and then mediated the drug carriers across cell membranes. Inspired by this strategy, we present here a steric protected and illumination activated tumor targeting drug carrier based on accessory-functionalized Pluronic P₁₂₃ micelles. The accessory is an ABA-typed amphiphilic polymer, which is shown in Figure 1. Biotin moiety, chosen as a model ligand, is hidden between hydrophobic core and hydrophilic shell of the micelles and the steric hindrance of the hydrophilic PEG shell can effectively restrict specific and non-specific contacts. Moreover, an *o*-nitrobenzyl group is located adjacently to biotin as a photo-cleavable junction. Upon illumination, this junction will disconnect and biotin moiety will be popped up to the micellar surface to facilitate the binding with the receptors on cell membrane (Scheme 1). Different from the strategy of directly removing PEG shells, the shielding effect in our system owing to the steric hindrance may disappear immediately without relying on the degree of degradation. More importantly, by utilizing the polymer to participate into the formation of nanoparticles with functionalized surface layer, this strategy could endow conventional nano-sized drug carriers with acute photo-triggered targeting function.

2. Results and Discussion

2.1. Synthesis and Characterization of Functional Accessory

The functional accessory, C₁₈-PEG-biotin-photo site-C₁₈ (CPB-p-C), was prepared by a similar procedure based on click chemistry according to our previous report.^[7] C₁₈-PEG-biotin-N₃ (CPBN₃) was synthesized by introducing azide-modified biotin moiety (Biotin-lys-N₃) into carbonyldiimidazole activated Brij 100. 1-(5-Methoxy-2-nitro-4-(octadecyloxy) phenyl) ethyl prop-2-ynylcarbamate (Alkyne-photo-C₁₈) was prepared based on the synthetic protocols reported by Holmes.^[22] Cu-catalyzed azide-alkyne cycloaddition (CuAAC) click chemistry was utilized to connect CPBN₃ and Alkyne-photo-C₁₈. As indicated by the ¹H NMR spectrum of CPB-p-C (Figure S1), nearly 100% of CPBN₃ was transformed into CPB-p-C according to the integration ratio of H atoms on the amide bond of biotin to that on the benzene ring. The successful synthesis of CPB-p-C was also proved by its gel permeation chromatography (GPC) trace and the change of FT-IR spectra before and after click chemistry (Figure S2 and Figure S3). The micelles prepared by Pluronic P₁₂₃ (PEG₂₀-PPG₇₀-PEG₂₀) were chosen as model drug carriers, which were extensively investigated as a type of long-circulating drug vehicle.^[23] To incorporate the 'targeting protection and stimuli activation' property to the delivery system,



Scheme 1. The mechanism of illumination-activated, tumor-targeting accessory for micelle-based drug carrier.

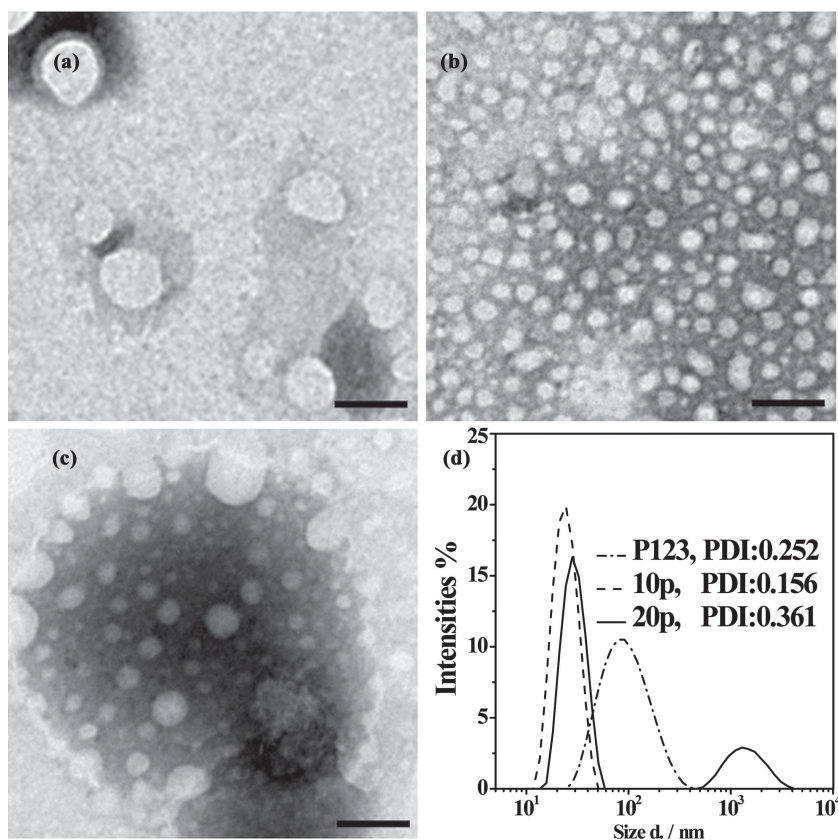


Figure 2. Transmission electron microscopy (TEM) images of a) P₁₂₃, b) 10p, and c) 20p micelles. The scale bar is 100 nm. d) the size and distribution of the micelles obtained by dynamic light scattering (DLS).

CPB-p-C was used as a functional accessory to decorate the P₁₂₃ micelles. CPB-p-C with a hydrophobic octadecyl chain and P₁₂₃ with a hydrophobic PPG chain could self-assemble in aqueous solution to form mixed micelles. The critical micelle concentrations (CMC) of CPB-p-C and P₁₂₃ were 32.3 mg/L and 33.8 mg/L, respectively (Figure S4). Two types of mixed micelles, 10p with CPB-p-C/P₁₂₃ weight ratio of 1/10 and 20p with CPB-p-C/P₁₂₃ weight ratio of 2/10, were prepared in this study. The sizes of both mixed micelles (10p: 23.4 ± 0.2 nm, 20p: 35.8 ± 0.3 nm) decreased in comparison with single P₁₂₃ micelles (75.6 ± 1.2 nm) due to the increase in the ratio of hydrophilic part to hydrophobic part (Figure 2). A smaller particle size would lead to more accumulation in tumor based on the enhanced permeability and retention (EPR) effect.^[24,25] The DLS experiments showed that the proportion of CPB-p-C also affected the size distribution of the mixed micelles. A small amount of large aggregations were formed in 20p, which was not found in 10p. With the increase of CPB-p-C amount, PEG chain tended to expand and form bridges among neighboring micelles, resulting in the formation of large aggregations.^[26] We also tested size and distribution change of the mixed micelles after UV-irradiation (Figure S5). 10p showed no obvious change. In contrast, the polydispersity index (PDI) value of 20p became much smaller, and some of large aggregations disappeared at the same time, which implied the damage of bridge-linked structure in 20p after UV-irradiation.

2.2. Steric Protection and Phototriggered Exposure of Targeting Ligands

In our study, the phototriggered cleavage of CPB-p-C was based on the property of *o*-nitrobenzyl group with photo-triggered rapid cleavage property.^[22] UV-vis spectrum of CPB-p-C showed two absorption peaks at 300 nm and at 345 nm (Figure 3A). After 5 min of UV-irradiation ($\lambda = 365$ nm, $I = 30$ mW/cm²), *o*-nitrobenzyl group was transformed to *o*-nitrosophenyl ethanone moiety. Thus the absorption maximum was red shifted to $\lambda = 382$ nm. The change of UV-vis spectrum of CPB-p-C was consistent with previous literatures.^[27] Detailed changes of UV-vis spectrum of CPB-p-C were shown in Figure S6. We further investigated the influence of steric hindrance on specific protein binding and whether the biotin ligands could be popped up onto the micellar surface after the cleavage of CPB-p-C. It is known that the complex of 4-hydroxyazobenzene-2'-carboxylic acid (HABA) and avidin has a strong absorption at 500 nm. Since the affinity between HABA and avidin is weaker than that between biotin and avidin, HABA can be easily replaced by biotin from HABA/avidin complex. Therefore, the contact between biotin and avidin could be quantitatively detected by the absorption decrease at 500 nm (see Experimental Section). By the HABA/avidin assays, we simulated the process of inactivating and activating targeting function. As shown in Figure 3B, only 5.2% of biotin was available to avidin in 10p, but nearly 11.6% of biotin could not be protected from avidin in 20p. It indicated that the outer PEG shell could sterically inactivate the targeting function, and the shield capability became weaker with the increase of CPB-p-C in the mixed micelles.

After irradiation for 5 min, there was about 7-fold increase of available biotin found in 10p as compared to the sample before irradiation, while the change in 20p was relatively smaller and a 2.8-fold increase was observed after irradiation. The change of binding capacity indicated that the shielding effect of PEG shell was destroyed due to the photo-triggered cleavage of CPB-p-C. The biotin moieties were popped up out of PEG shell to bind avidin freely. It was worth noting that the photo-activated binding capacity was still lower than that of the positive controls. The introduction of triazole ring by click chemistry might increase the hydrophobic contact with the micellar core, which restrained the chain unfolding of PEG.

After irradiation for 5 min, there was about 7-fold increase of available biotin found in 10p as compared to the sample before irradiation, while the change in 20p was relatively smaller and a 2.8-fold increase was observed after irradiation. The change of binding capacity indicated that the shielding effect of PEG shell was destroyed due to the photo-triggered cleavage of CPB-p-C. The biotin moieties were popped up out of PEG shell to bind avidin freely. It was worth noting that the photo-activated binding capacity was still lower than that of the positive controls. The introduction of triazole ring by click chemistry might increase the hydrophobic contact with the micellar core, which restrained the chain unfolding of PEG.

2.3. Phototriggered Cellular Uptake

Phototriggered cellular uptake of the mixed micelles was examined in Human cervical cancer cells (HeLa cells) with over-expression of biotin receptors^[28] by confocal laser scanning microscopy (CLSM). P₁₂₃ was labeled with fluorescein

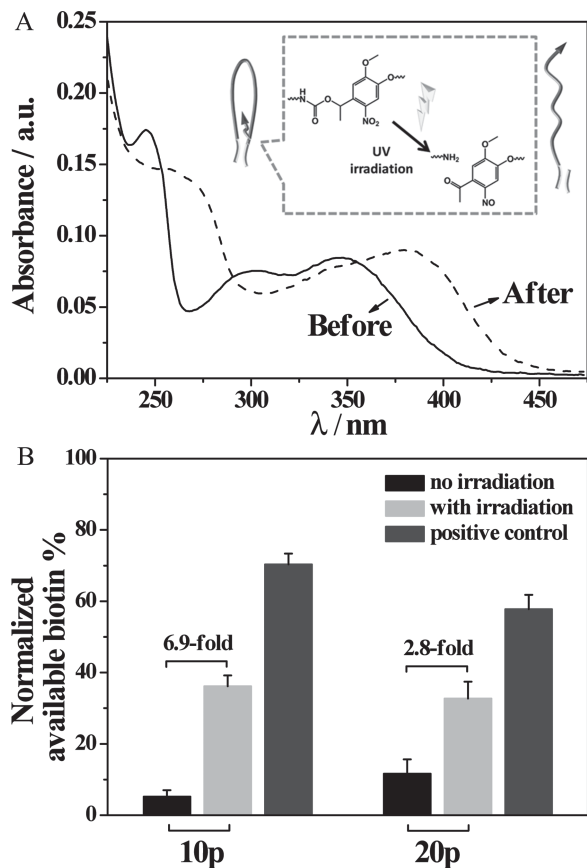


Figure 3. A) The UV-vis absorption spectra of CPB-p-C in PBS before and after UV-irradiation (5 min, $I = 30 \text{ mw/cm}^2$). B) Results of HABA/avidin assay of 10p and 20p before and after UV-irradiation (5 min, $I = 30 \text{ mw/cm}^2$). Positive controls were 10+ and 20+ ($W_{P123}/W_{CPBN3} = 10/1$ and $10/2$), respectively. The amounts of biotin available in 10p and 20p were normalized to their theoretical amount of biotin in CPB-p-C, respectively; and the amounts of biotin available in 10+ and 20+ were normalized to their theoretical amount of biotin in CPBN₃, respectively. The amounts of biotin in CPB-p-C and CPBN₃ were calculated by ¹H NMR.

isothiocyanate (FITC) to obtain P₁₂₃-FITC, and the mixed micelles were prepared by mixing P₁₂₃-FITC solution and CPB-p-C solution. Then the HeLa cells were treated with these mixed micelles for 30 min with or without UV-irradiation (30 s of irradiation with 30 s of nonirradiation interval between light irradiations for total 5 min). As shown in Figure 4, 10p and P₁₂₃-FITC micelles exhibited similar cellular uptake, which implied that introducing a small amount of functional accessories did not lead to additional unexpected cellular uptake. It is noted that a side effect was observed when the amount of CPB-p-C increased. As compared to negative control, the cells treated with 20p showed enhanced green fluorescence although there was no light stimulus. According to the results of HABA/Avidin assay, we believed that the unexpected cellular uptake was related with the amount of unprotected biotin moieties in 20p. Upon UV-irradiation, no change could be observed in the HeLa cells treated with P₁₂₃ micelles but obviously enhanced green fluorescence could be found

in the other two samples. The shielded biotin moieties were re-exposed on the surface of micelles due to the photo-triggered cleavage of CPB-p-C. The enhanced cellular internalization of the mixed micelles of P₁₂₃-FITC was due to the biotin receptor-mediated endocytosis.

Quantitative characterization of cellular uptake was performed by flow cytometry (Figure 4E). There was no significant difference in intracellular fluorescence intensities between the cells treated with 10p and P₁₂₃-FITC micelle. A 2.2-fold increase of fluorescence could be found in cells treated with 20p. Upon light stimulation, the sample of P₁₂₃ micelle did not show significant difference but 10p and 20p with the functional accessory CPB-p-C exhibited 5.2- and 6.5-fold increase in cellular uptake, respectively. Obviously, the increase of fluorescence intensities was correlated with the amount of free biotin moieties on the micelle surface. It was noted that fluorescence intensities of both samples after irradiation was close to that of the positive controls although there were only about 50% of biotin moieties were free to receptors in 10p and 20p after UV-irradiation. It is known that not all ligands on micelles are required for effective cell targeting.^[29] The excessive addition of functional accessory did not further improve phototriggered uptake of fundamental micelles but led to un-specific intracellular accumulation. So 10p seems to be a better formula than 20p.

2.4. Determination of Endocytosis Pathways

It is well known that biotinylated conjugates could cross cancer cell membranes by a ligand receptor-mediated process,^[28,30] which was known as a clathrin-mediated endocytosis. In our system, biotin moieties underwent a process of position change from micellar inner core to micellar outer layer upon light stimulation. Correspondingly, cellular uptake of the mixed micelles increased as the exposure of biotin ligands. To further understand the role of biotins, we investigated the mechanism involved in the endocytosis of the mixed micelles before and after UV-irradiation. Three inhibitors of endocytosis, chlorpromazine, amiloride and genistein, were used to inhibit clathrin-mediated endocytosis, macropinocytosis and caveolin-mediated endocytosis, respectively (Figure 5). Genistein and amiloride showed much weaker influence on cellular uptake of these mixed micelles than chlorpromazine, implying that the clathrin-mediated endocytosis was the primary endocytosis pathway for P₁₂₃ based mixed micelles. Although the cellular internalization of 10p was mainly inhibited by chlorpromazine regardless of illumination, the cellular uptake of 10p with activated targeting function was more dependent on clathrin-mediated endocytosis than the one without illumination. Before UV-irradiation, about 25% of cellular internalization of 10p was inhibited by chlorpromazine and this value increased to 53% after UV-irradiation. It indicated that biotin-receptor mediated endocytosis was the most important endocytic pathway in this photo-activated targeting delivery. In contrast, chlorpromazine decreased the cellular internalization of 20p by 57% and 48% with or without UV-irradiation, respectively. It implied that more unprotected biotin ligands on 20p resulted in more unexpected clathrin-mediated endocytosis

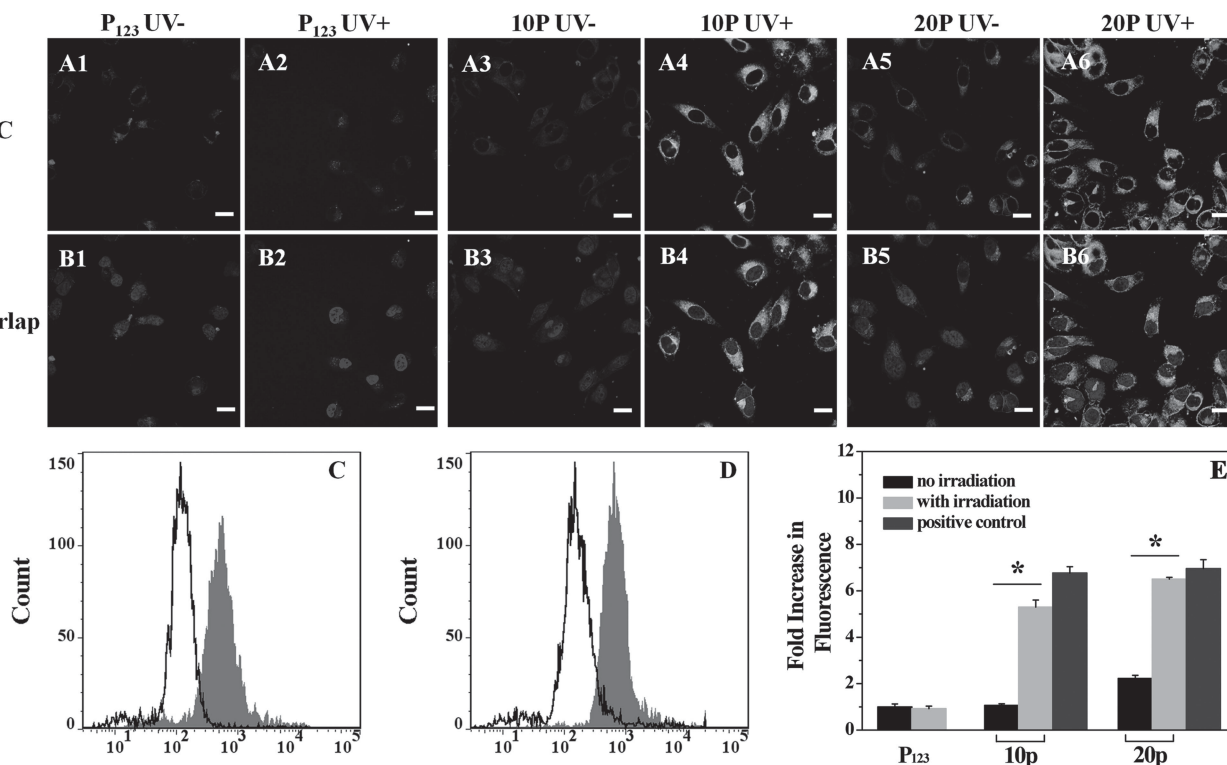


Figure 4. The CLSM images of HeLa cells treated with mixed micelles before and after UV-irradiation. The HeLa cells were incubated with FITC-labeled P₁₂₃, 10p and 20p for 30 min at 37 °C. Then the cell nuclei were stained with Hoechst 33258. For photo-triggered experiments, the cells were exposed to UV-irradiation (30 s of irradiation with 30 s of nonirradiation interval between light irradiations) for total 5 min. A1-A6 were the green fluorescence channel and B1-B6 were the overlap of green and blue channel. The scale bar is 20 μm. Flow cytometry analysis of FITC-labeled 10p (C) and 20p (D) exposed to HeLa cells before (black line) and after UV-irradiation (gray filled). Quantitative comparison of photo-triggered cell uptake of FITC-labeled mixed micelles (**p* < 0.05). The negative control was P₁₂₃ and the positive controls were 10+ and 20+.

before UV-irradiation, which also confirmed our previous speculation.

2.5. In Vitro Photocontrolled Drug Release and Cytotoxicity

Next these mixed micelles were used to encapsulate anti-tumor drug doxorubicin (DOX) to study the photocontrolled targeted drug delivery. The amount of DOX loaded in these P₁₂₃ based micelles was shown in Table S1. We first evaluated the drug release behavior of the mixed micelles with or without UV irradiation. As shown in Figure 6, all samples showed relatively fast release of DOX at the initial stage and 10p exhibited slightly quicker release of DOX than P₁₂₃/brij100 (10/1) in 24 h. Upon UV irradiation, the drug release behavior of 10p was suppressed and about 45.8% of DOX was finally released after 24 h. This value was about 50.3% in the same formulation but without UV irradiation. Considering the negligible change of drug release behavior of P₁₂₃/brij100 (10/1) after irradiation (Figure 6A), we could conclude that the bended structure of CPB-p-C in the mixed micelles might increase drug release from the mixed micelles before irradiation. After UV irradiation, the photo-cleavage of *o*-nitrobenzyl group in CPB-p-C decreased the number of PEG chains on the surface of the micelles (two became one). Thus some

hydrophilic channels^[31] for drug release were shut down, resulting in the decreased release of DOX. Similar trend was observed in the drug release profile of 20p and the amount of released DOX from 20p was decreased from 56.1% to 48.8% upon irradiation after 24 h. We noted that the total amount of released DOX from 20p was more than that of 10p. It also could be explained by the increase of hydrophilic channels in 20p.

Finally, in vitro photocontrolled targeted drug delivery was evaluated by MTT assay in HeLa cells. As shown in Figure 7, before UV-irradiation, the cells treated with 10p showed similar cytotoxicity to that of negative control, which meant effective protection of PEG shells in 10p. After UV-irradiation, there was a dramatic cell viability decrease and IC₅₀ of 10p dropped from 0.261 to 0.121 μg/mL. As shown in Figure 7B, compared to 10p, 20p showed a stronger tumor cell inhibition due to the increased amount of CPB-p-C, which caused a higher cytotoxicity in HeLa cells even without UV-irradiation. After UV-irradiation, the IC₅₀ value of 20p dropped to 0.099 μg/mL, which was close to that of positive control (IC₅₀: 0.072 μg/mL). It was worth noting that the improvement on cytotoxicity of 10p or 20p after UV-irradiation was less obvious than the results of cellular uptake shown in Figure 4E. According to the results in Figure 6, a fast drug release from P₁₂₃/CPB-p-C based micelles without irradiation was found, which might override the effect

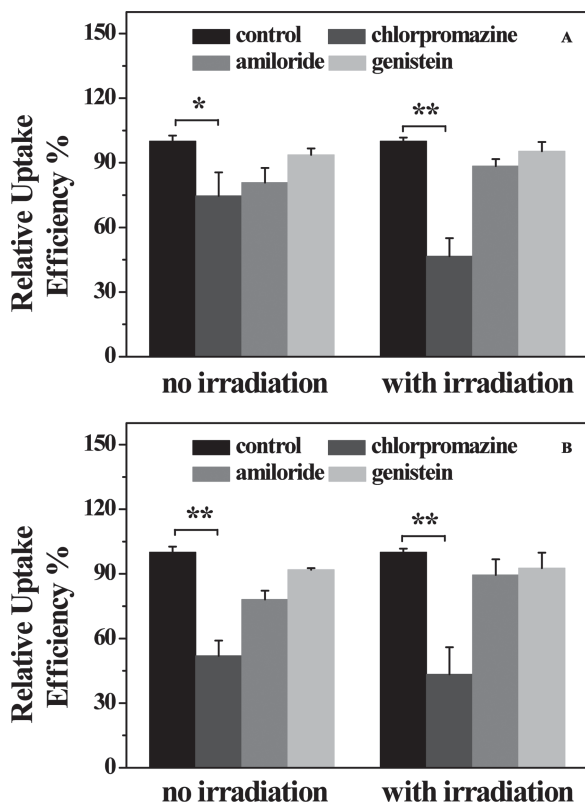


Figure 5. Relative uptake efficiency of 10p (A) and 20p (B) in HeLa cells in the presence of various endocytosis inhibitors with and without UV-irradiation. Chlorpromazine, amiloride, and genistein were used as inhibitors for clathrin-mediated endocytosis, macropinocytosis, and caveolin-mediated endocytosis, respectively. The results obtained by flow cytometry. * $p < 0.05$, ** $p < 0.01$.

of cellular uptake, and finally reduced the phototriggered cytotoxicity.

We further evaluated the cytotoxicity of blank micelles and UV irradiation on HeLa cells. It was reported that Pluronic P₁₂₃ micelles displayed certain cytotoxicity at high concentration due to the cytostatic action of Pluronic micelles.^[32] However, a low dose of P₁₂₃ might limit its drug loading content (DOX < 0.3% w/w, Table S1) and affect its micellar formation (CMC_{P123} = 33.8 mg/L). Therefore, we set the maximum dose of P₁₂₃ at 200 µg/mL based on the balance between its concentration and toxicity. HeLa cells showed nearly 70% of cell viability at this concentration for 24 h (Figure S7). It should be noted that the concentration of mixed micelles at DOX concentration of 0.05 µg/mL was little lower than the CMC of P₁₂₃. However, we still observed the photo-triggered cell apoptosis. We speculated that the mixing of P₁₂₃ and CPB-p-C and the encapsulation of hydrophobic drugs might improve the stability of micelle.^[33] Except P₁₂₃, the other materials and UV irradiation were less toxic at the dose used in this work. It proved again that it would safe to endow conventional nano-sized drug carriers with acute photo-triggered targeting function by adding small amount of functional accessories.

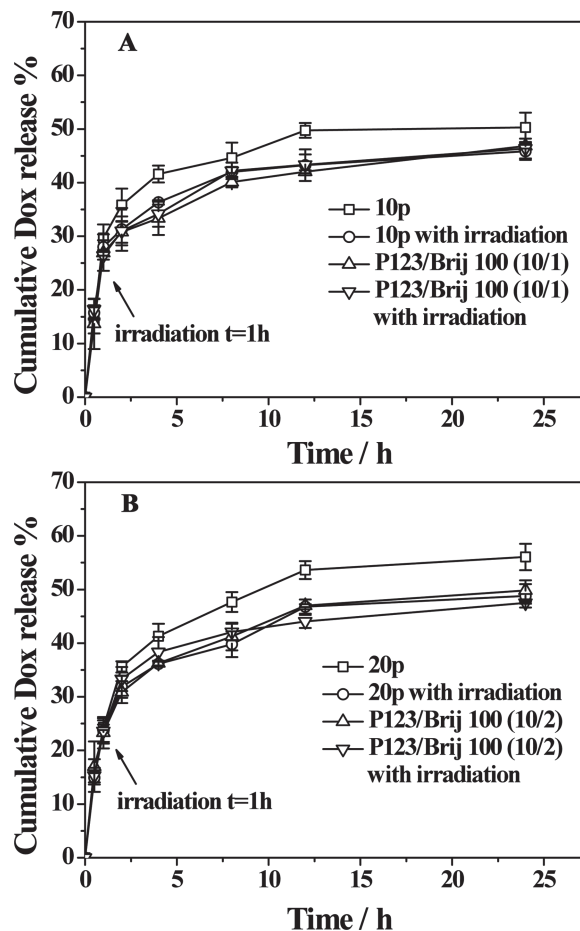


Figure 6. The cumulative DOX release from (A) 10p and (B) 20p in PBS (0.1 M) at 37 °C. The samples were exposed to UV-irradiation ($I = 30 \text{ mW/cm}^2$) for 5 min after 1 h of shaking.

The facile strategy to achieve 'targeting protection and stimuli activation' property in this study is applicable to other micelle based drug carriers by using the functional accessories with similar structures. To further improve the compatibility of the functional accessories for other drug carriers, we can change the type or the molecular weights of the hydrophobic parts. We may also introduce different types of targeting ligands for various cancerous cell lines. All these changes can be easily achieved by the 'click chemistry' based synthesis route. Moreover, o-nitrobenzyl groups used here can respond to near infrared light sources based on two-photon absorption,^[34,35] which will enhance the in vivo applications of our 'steric hindrance protection and illumination activated' tumor targeting drug delivery systems.

3. Conclusion

We report here an accessory to endow traditional micelle-based drug carriers with illumination-activated tumor specific intracellular drug delivery capacity. Due to the folded PEG structure in the mixed micelles, the targeting function of CPB-p-C was

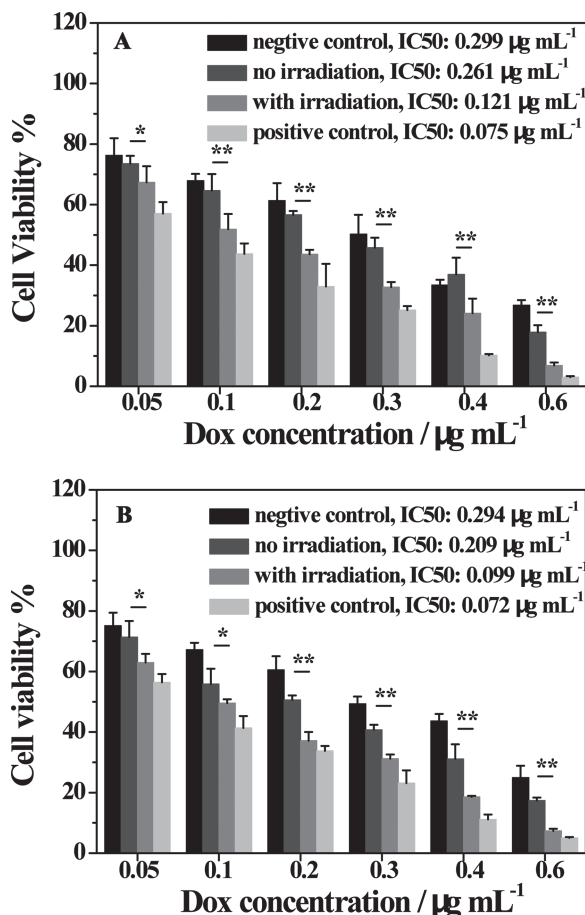


Figure 7. Cell viability studies of HeLa cells incubated individually with DOX-loaded 10p (A) and 20p (B) for 24 h. Negative controls were DOX loaded P₁₂₃/Brij100 mixed micelles and positive controls were DOX loaded P₁₂₃/CPBN₃ mixed micelles (w/w = 10/1 for 10p and 10/2 for 20p, respectively). *p < 0.05, **p < 0.01. The maximum amount of DOX loaded micelles (at C_{DOX} = 0.6 $\mu\text{g/mL}$) used in MTT assays were 215.8, 226.4, 212.0, 229.0, 236.2 and 232.6 $\mu\text{g/mL}$, which corresponded to DOX loaded 10p, 10+, P₁₂₃/Brij 100 (10/1), 20p, 20+, and P₁₂₃/Brij 100 (10/2) micelles, respectively.

effectively suppressed by PEG shells before UV-irradiation. After UV-irradiation, the cleavage of o-nitrobenzyl groups in CPB-p-C led to the stretch of PEG chains, resulting in the exposure of biotin moieties. In vitro studies showed that CPB-p-C indeed improved the intracellular uptake of mixed micelles by photo stimulus and further enhanced the cytotoxicity of DOX-loaded micelles in HeLa cells. The strategy developed in this study is applicable to other micelle based drug carriers to achieve 'targeting protection and stimuli activation' property.

4. Experimental Section

Materials: Acetovanillone, 1-bromooctadecane, sodium nitrite, nitric acid (65%–68%), sodium borohydride (NaBH₄), 1,1'-carbonyldiimidazole (CDI), 2-propynylamine and N,N,N',N',N''-pentamethyl diethylenetriamine (PMDETA) were purchased from Aladdin-reagent (China) and used as received. CuBr, Brij 100 (C18-

PEG₁₀₀-OH, Mn: 4670), Pluronic P₁₂₃ (PEG₂₀-PPG₇₀-PEG₂₀, Mn: 5800), Avidin, chlorpromazine, amiloride and genistein were purchased from Sigma-Aldrich and used as received. Hydroxyazobenzene-2-carboxylic acid (HABA) and Fluorescein isothiocyanate isomer I (FITC) were purchased from Alfa aesar and used as received. Merrifield Resin (1.0–1.1 mmol/g) was purchased from GL Biochem (Shanghai) Ltd. Doxorubicin hydrochloride (Dox-HCl) was purchased from Zhejiang Hisun Pharmaceutical Co., Ltd. (China). Bovine serum albumin (BSA), Dubelcco's Modified Eagle's Medium (DMEM), penicillin–streptomycin, trypsin, and phosphate-buffered saline (PBS), and 3-(4,5-dimethylthiazol-2-yl)-2,5-diphenyltetrazolium bromide (MTT) were purchased from GIBCO Invitrogen Corporation. All the organic solvent used here was dried and re-distilled by common method.

1-(3-Methoxy-4-(octadecyloxy)phenyl) Ethanone (1): A slurry of acetovanillone (5.12 g, 30.8 mmol), 1-bromooctadecane (11.31 g, 33.9 mmol), and K₂CO₃ (6.38 g, 46.2 mmol) in 50 mL of dimethylformamide (DMF) and acetone (v/v = 1/1) was stirred at 60 °C overnight. Then the mixture was poured into excess distilled water to remove salts. The precipitate was collected and dissolved in 200 mL of DCM. The solution was washed with distilled water, brine and dried over anhydrous Na₂SO₄, then concentrated. The crude product was recrystallized with CH₃OH to yield white solid (1). Yield: 12.46 g (96.7%). ¹H NMR (300 MHz, CDCl₃) δ : 7.56–7.50 (m, 2H), 6.88 (s, 1H), 4.07 (t, 2H), 3.92 (s, 3H), 2.56 (s, 3H), 1.88 (m, 2H), 1.46 (m, 2H), 1.26 (m, 28H), 0.88 (d, 3H). ¹³C NMR (75 MHz, CDCl₃) δ : 197.0, 153.3, 149.5, 130.5, 123.5, 111.3, 110.7, 69.3, 56.3, 32.2, 30.4, 30.0, 29.7, 29.3, 26.4, 26.2, 23.0, 14.4.

1-(5-Methoxy-2-nitro-4-(octadecyloxy)phenyl) Ethanone (2): A mixture of (1) (6.28 g, 15.0 mmol) and sodium nitrite (0.14 g, 2.0 mmol) in 30 mL of DCM was stirred at room temperature. Nitric acid (65–68%, 4.36, 45.0 mmol) in 10 mL of DCM was added dropwise to the mixture and the reaction was chilled in an ice-water bath. After addition, the emulsion was kept stirring at room temperature for 6 h. Then the mixture was poured into water and extracted with CH₂Cl₂. The organic layer was combined and washed with saturated NaHCO₃, distilled water, brine and dried over anhydrous Na₂SO₄. The solvent was concentrated and the residue was purified by chromatography on silica gel by eluting petroleum ether with 15% of ethyl acetate. The product was obtained as yellow crystal (2). Yield: 4.41 g (63.5%). ¹H NMR (300 MHz, CDCl₃) δ : 7.59 (s, 1H), 6.77 (s, 1H), 4.09 (t, 2H), 3.96 (s, 3H), 2.49 (s, 3H), 1.88 (m, 2H), 1.47 (m, 2H), 1.26 (m, 28H), 0.87 (d, 3H). ¹³C NMR (75 MHz, CDCl₃) δ : 200.2, 154.3, 149.3, 138.5, 132.6, 108.8, 107.8, 69.9, 56.8, 32.1, 30.5, 29.9, 29.7, 29.5, 28.9, 26.0, 22.9, 14.3.

1-(5-Methoxy-2-nitro-4-(octadecyloxy)phenyl) Ethanol (3): A solution of (2) (1.50 g, 3.23 mmol) in 50 mL of THF was mixed with NaBH₄ (263 mg, 6.95 mmol) at room temperature. The reaction mixture was stirred for 24 h and then partitioned between EtOAc and saturated NH₄Cl. The combined organic phase was dried over anhydrous Na₂SO₄ and concentrated under vacuum. The residue was purified by chromatography on silica gel by eluting (20% ethyl acetate/petroleum ether to 30% ethyl acetate/petroleum ether) to give (3) as yellow solid. Yield 1.34 g (88.9%). ¹H NMR (300 MHz, CDCl₃) δ : 7.88 (dd, 1H), 7.71 (d, 1H), 6.88 (d, 1H), 4.08 (t, 2H), 3.92 (s, 3H), 1.86 (m, 2H), 1.45 (m, 2H), 1.23 (m, 28H), 0.85 (d, 3H). ¹³C NMR (75 MHz, CDCl₃) δ : 154.5, 149.3, 141.4, 118.0, 110.9, 106.8, 69.7, 56.5, 32.2, 29.9, 29.8, 29.8, 29.6, 29.1, 26.1, 22.9, 14.4.

1-(5-Methoxy-2-nitro-4-(octadecyloxy)phenyl) Ethanol (Alkyne-p-C, 4): A solution of (3) (1.0 g, 2.38 mmol) in 20 mL of DCM was mixed with 1,1'-carbonyldiimidazole (CDI, 0.77 g, 4.75 mmol) at room temperature. The reaction was stirred for 4 h and then partitioned between DCM and distilled water. The combined organic phase was washed twice with distilled water, dried over anhydrous Na₂SO₄ and concentrated under vacuum. The residue was directly used in the next step without further purification. The aforementioned residue was resolved in 15 mL of DCM and added dropwise with a solution of 2-propynylamine (0.26 g, 4.72 mmol) in 5 mL of DCM. The reaction was stirred overnight at room temperature and then washed twice with distilled water, dried over anhydrous Na₂SO₄ and concentrated under vacuum. The residue

was purified by column chromatography (SiO₂, eluent: petroleum ether with 15% of ethyl acetate). The (4) was obtained as yellow powder. Yield: 0.85 g (72.6%). ¹H NMR (300 MHz, CDCl₃) δ: 7.57 (s, 1H), 7.00 (s, 1H), 6.41 (m, 1H), 5.34–5.17 (m, 1H), 4.04 (t, 2H), 3.96 (m, 5H), 2.23 (s, 1H), 1.85 (m, 2H), 1.60 (d, 3H), 1.45 (m, 2H), 1.26 (m, 28H), 0.88 (t, 3H). ¹³C NMR (75 MHz, CDCl₃) δ: 155.1, 154.2, 147.7, 139.8, 133.6, 108.9, 108.2, 79.8, 71.9, 69.7, 56.5, 32.1, 31.0, 29.9, 29.8, 29.8, 29.6, 29.1, 27.4, 26.1, 24.6, 22.9, 22.4, 14.3.

Biotin-lys(PEG-C18)-N3 (5): According to a previous publication,^[7] biotin-lys(PEG-C18)-N3 was synthesized as follows. Briefly, H-lys(Boc)-OH was reacted with biotin *N*-hydroxy succinimide ester (biotin-NHS) in the presence of triethylamine to form biotin-lys(Boc)-OH. After the carboxyl group was reacted with aminopropylazide, the Boc group was removed by adding excess TFA (90% in DCM) to obtain free amino group. Finally, biotin-lys(PEG-C18)-N3 was obtained by the reaction between biotin-lys-N3 and carbonyl imidazole activated Brij 100.

Alkyne-resin: Merifield's resin (1 g, 1.0–1.1 mmol), K₂CO₃ (6.9 g, 0.050 mol), and propargyl alcohol (2.8 g, 0.050 mol) were added in 40 mL of DMF and the resulting mixture was stirred at 110 °C for 48 h. The obtained resin was washed several times with water and THF, respectively. The alkyne-resin was collected by filtration and dried under vacuum. FTIR (cm⁻¹): 2330 (HC≡C–CH₂) and 3300 (HC≡C–CH₂).

CPB-p-C: Biotin-lys(PEG-C18)-N3 (0.5 g, 0.10 mmol) and 4 (0.16 g, 0.29 mmol) were dissolved in 2 mL of DMF. After three freeze-pump-thaw cycles, PMDETA (5.2 mg, 0.03 mmol) and CuBr (4.3 mg, 0.03 mmol) were added and the solution was stirred under Ar atmosphere at 35 °C for 48 h. Then the solution was frozen under liquid nitrogen and alkyne-resin (0.2 g, ~0.2 mmol), fresh PMDETA (17.3 mg, 0.1 mmol) and CuBr (14.3 mg, 0.1 mmol) were added. After three freeze-pump-thaw cycles again, the solution was stirred for another 48 h. Finally, the reaction was stopped and the solution was diluted with THF. After passing through a short alumina column to eliminate the copper and resin, the product was obtained by three times of precipitation in excess ice-cooled ethyl ether and dried under vacuum.

Polymer Characterization: ¹H NMR spectra were recorded at 300 MHz on a Mercury VX-300 spectrometer by using tetramethylsilane (TMS) as the internal reference. ¹³C-NMR spectra were recorded at 75 MHz with the solvent carbon signal as reference. Infrared spectra were recorded on a Nicolet Avator 360 FT-IR spectrometer. The molecular weight and molecular weight distribution of the polymer were determined by gel permeation chromatography equipped with a Waters 2690 separation module and a Waters 2410 refractive index detector. DMF was used as eluent at a flow rate of 0.5 mL min⁻¹ with the temperature maintained at 30 °C and the results were calibrated against with polyethylene glycol standards.

Micelle Preparation and Characterization: In this work, all the micelle solutions were prepared by diluting pre-made high concentration micelle stocks and kept in 37 °C for 24 h to reach equilibrium before use. For example, 10p (P₁₂₃: 1 mg/mL) was prepared as follows: equal volumes of P123 micelle (10 mg/mL) and CPB-p-C (1 mg/mL) were mixed and then diluted to 5-fold volume. Size and distribution measurements of the micelles were performed on a Nano-ZSEN3600 (Malvern) instrument. Critical micelle concentration (CMC) of CPB-p-C and P₁₂₃ were collected by the pendant drop method for measuring surface tension for a series of sample solutions. An optical contact angle measuring device (OCA 30, Dataphysics) was used to measure the surface tension. The CMC was estimated as the intersection when extrapolating the surface tension at low and high concentration regions. Transmission electron microscopy images (TEM) were obtained using a JEM-100CXII transmission electron microscope. A drop of micelle solution was placed onto a copper grid with carbon film and then stained with phosphotungstic acid. The TEM images were observed at an acceleration voltage of 200 keV.

Photodegradation: The photo-triggered detachment of CPB-p-C was performed in aqueous phase (phosphate buffered saline (PBS), 0.1 M) and organic phase (1,4-dioxane). CPB-p-C solution was added into a sealed quartz cuvette and placed under UV lamp (FC-100/F, Spectronics) at an intensity of I = 10 mW/cm² (organic phase) or 30 mW/cm²

(aqueous phase). At the fixed time intervals, the UV spectrum of cpb-p-C solution was recorded on UV-Vis spectrophotometer.

HABA/Avidin Assay: As described in a previous publication,^[7] the HABA/avidin assay was performed according to protocols reported by Wooly.^[36] The HABA solution was prepared by dissolving 24.2 mg of 4-hydroxyazobenzene-2-carboxylic acid (0.1 mmol) in 10 mL of aqueous sodium hydroxide solution (10 mM). Then the HABA/avidin solution was made by dissolving 5.0 mg of avidin in 9.7 mL of 50 mM PBS with 50 mM NaCl (pH = 7.2), followed by adding HABA solution (300 μL). 10p or 20p (C_{P123} was fixed at 10 mg/mL) was added into a sealed quartz cuvette and placed under the UV lamp at an intensity of I = 30 mW/cm² for 5 min. Aliquots (22.2 μL) were taken out at the regular time intervals and mixed with 200 μL of HABA/avidin solution. The final mixtures were kept at 37 °C for 6 h to reach equilibrium. 200 μL of the mixtures were transferred into a 96-well plate and read by UV/Vis microplate spectrophotometer (Multiskan GO, Thermo Fisher).

Cellular Uptake by CLSM: Cell internalization was observed on confocal laser scanning microscopy (CLSM, Nikon C1-si). All the mixed micelles used in this measurement were based on fluorescein isothiocyanate (FITC) modified P₁₂₃ (concentration: 0.1 mg/mL). HeLa cells were seeded in a 35 mm cell culture dish with glass bottom and incubated at 37 °C for 24 h. The samples in DMEM with 10% fetal bovine serum (FBS) were added to replace the medium. After 30 min of incubation, the medium was removed and the cells were washed three times with PBS. The nuclear was stained with Hoechst 33258 and the cells were fixed with 4 wt% formaldehyde in PBS for 20 min at room temperature. A drop of mounting media (10% PBS, 90% glycerol) were added to mount the cells. For UV irradiation measurement, the cell culture dish was exposure to the UV light in an alternate way (30 s of irradiation with 30 s of nonirradiation interval between light irradiations) for total 5 min of irradiation at an intensity of I = 30 mW/cm² and incubated for another 20 min. The fluorescence was examined under excitation at 405 nm for Hoechst 33258 and 488 nm for FITC.

Flow Cytometry: HeLa cells were seeded in 6-well plates and incubated for 24 h at 37 °C with 5% CO₂. The samples in DMEM with 10% fetal bovine serum (FBS) were added to replace the medium and incubated for 30 min. For UV irradiation measurement, the 6-well plate was exposed to UV light in an alternate way (30 s of irradiation with 30 s of nonirradiation interval between light irradiations) for total 5 min of irradiation at an intensity of I = 30 mW/cm² and incubated for another 20 min. Then the medium was removed and the cells were washed with PBS (4 °C) for three times, harvested by 0.25% (w/v) trypsin-0.03% (w/v) EDTA solution. The cells were pelleted by centrifuge (1000 rpm for 5 min), resuspended in fresh PBS and analyzed on a flow cytometer (FACSAriaTMIII). Flow cytometry analysis was used to evaluate the endocytosis pathways of 10p and 20p mixed micelles with and without UV irradiation. The HeLa cells were pre-incubated with endocytosis inhibitors (inhibitor of clathrin-mediated endocytosis: chlorpromazine hydrochloride (30 μg/mL); inhibitor of caveolin-mediated endocytosis: genistein (15 μg/mL); inhibitor of macropinocytosis: amiloride (133 μg/mL) for 30 min at 37 °C. Then the mixed micelles in complete medium with corresponding concentration of inhibitors were added to replace the medium. After the same procedures as cell uptake, the cells were analyzed on a flow cytometer.

Drug Encapsulation: DOX was loaded into the micelles as a model anti-tumor drug by o/w emulsion method. Typically, 0.1 mg of doxorubicin hydrochloride was added into CHCl₃ (3 mL) and solubilized by adding two equivalents of triethylamine under sonication. The above solution was added into a stirred mixed micelle solution (C_{P123}: 0.5 mg/mL, volume: 60 mL), to form o/w emulsion. The emulsion was kept stirring overnight to evaporate CHCl₃ and then dialyzed against with deionized water to get rid of free DOX and triethylamine salt. Then the mixture was passed through a 0.45 μm filter and lyophilized (2 mL per one tube). The loaded content of DOX was determined by fluorescence emission spectroscopy. The excitation wavelength was set as 480 nm and the emission wavelength was 560 nm with 5 nm of slit width. The Loading content (LC) and loading efficacy (LE) were calculated by the following equations.

$$\text{LC\%} = (\text{weight of the drug in micelles}) / (\text{weight of the drug loaded micelles}) \times 100\%$$

$$\text{LE\%} = (\text{weight of the drug in micelles}) / (\text{weight of the feeding drug}) \times 100\%$$

In vitro Release of DOX-Loaded Micelles: Typically, the lyophilized DOX-loaded micelles were resolved in PBS (2 mL, 0.5 mg/mL) and transferred into a dialysis bag (Mw cutoff: 3500). The dialysis bag was immersed into 20 mL of PBS dialysate (0.1 M, pH 7.4) and then shaken at 37 °C. At the preset intervals, 2 mL of solution was withdrawn from the release medium and replaced with equal volume of fresh PBS. As to the photo-triggered experiments, the dialysis bag was exposed to 5 min of UV irradiation after 1 h of shaking. The DOX content released from micelles was determined by fluorescence emission spectroscopy.

Cytotoxicity: The cytotoxicity assessment was carried out in Hela cells by using MTT assay. 100 μL of cell suspension containing 5×10^3 cells were seeded into each well of a 96-well plate and incubated at 37 °C with 5% CO_2 for 24 h. Then the cells were treated with samples at various concentrations and carried out a further incubation for 24 h. For UV irradiation measurement, the cells were exposed to UV light in an alternate way (30 s with and 30 s without irradiation) for total 5 min of irradiation at an intensity of $I = 30 \text{ mW/cm}^2$ and incubated for 24 h in incubator. Then the medium in each well was replaced with 200 μL of fresh mediums and 20 μL of MTT solution in PBS (5 mg/mL). After 4 h of incubation, the medium was carefully removed and replaced by 100 μL DMSO to solve the purple crystals. When the purple solution was homogeneous, the absorbance at 570 nm was recorded by a microplate reader (Multiskan GO, Thermo Fisher). Cell viability was calculated as follows.

$$\text{Cell viability(\%)} = (\text{A}_{\text{treated}} - \text{A}_{\text{blank}}) / (\text{A}_{\text{control}} - \text{A}_{\text{blank}}) \times 100\%$$

The data are shown as the average value \pm standard deviation.

Statistics: All data collected were presented as mean \pm standard deviation based on three or more experiments. A one-way analysis of variance (ANOVA), followed by a Student's *t*-test was employed to compare data sets using *p* values of 0.05 or less to determine statistical significance.

Supporting Information

Supporting Information is available from the Wiley Online Library or from the author.

Acknowledgements

This work was financially supported by National Basic Research Program of China (2011CB606202), the Natural Science Foundation of Hubei Province (2012FFB04327) and National Natural Science Foundation of China (20704032 and 21374082).

Received: April 18, 2013

Revised: September 14, 2013

Published online: December 2, 2013

- [1] V. P. Torchilin, A. N. Lukyanov, Z. G. Gao, B. Papahadjopoulos-Sternberg, *Proc. Natl. Acad. Sci. USA* **2003**, *100*, 6039.
 [2] K. S. Soppimath, L. H. Liu, W. Y. Seow, S. Q. Liu, R. Powell, P. Chan, Y. Y. Yang, *Adv. Funct. Mater.* **2007**, *17*, 355.

- [3] L. M. Pan, Q. J. He, J. N. Liu, Y. Chen, M. Ma, L. L. Zhang, J. L. Shi, *J. Am. Chem. Soc.* **2012**, *134*, 5722.
 [4] S. Dhar, F. X. Gu, R. Langer, O. C. Farokhzad, S. J. Lippard, *Proc. Natl. Acad. Sci. USA* **2008**, *105*, 17356.
 [5] E. S. Lee, Z. Gao, Y. H. Bae, *J. Controlled Release* **2008**, *132*, 164.
 [6] J. Z. Du, T. M. Sun, W. J. Song, J. Wu, J. Wang, *Angew. Chem. Int. Ed.* **2010**, *49*, 3621.
 [7] Z. Yuan, Z. Que, S. Cheng, R. Zhuo, F. Li, *Chem. Commun.* **2012**, *48*, 8129.
 [8] C. Ding, J. Gu, X. Qu, Z. Yang, *Bioconjugate Chem.* **2009**, *20*, 1163.
 [9] E. Jin, B. Zhang, X. Sun, Z. Zhou, X. Ma, Q. Sun, J. Tang, Y. Shen, E. Van Kirk, W. J. Murdoch, M. Radosz, *J. Am. Chem. Soc.* **2013**, *135*, 933.
 [10] X. Z. Yang, J. Z. Du, S. Dou, C. Q. Mao, H. Y. Long, J. Wang, *ACS Nano* **2011**, *6*, 771.
 [11] C. Y. Quan, J. X. Chen, H. Y. Wang, C. Li, C. Chang, X. Z. Zhang, R. X. Zhuo, *ACS Nano* **2010**, *4*, 4211.
 [12] Z. X. Zhou, Y. Q. Shen, J. B. Tang, M. H. Fan, E. A. Van Kirk, W. J. Murdoch, M. Radosz, *Adv. Funct. Mater.* **2009**, *19*, 3580.
 [13] N. Fomina, C. McFearin, M. Sermsakdi, O. Edigin, A. Almutairi, *J. Am. Chem. Soc.* **2010**, *132*, 9540.
 [14] G. C. R. Ellis-Davies, *Nat. Methods* **2007**, *4*, 619.
 [15] S. Tamesue, Y. Takashima, H. Yamaguchi, S. Shinkai, A. Harada, *Angew. Chem. Int. Ed.* **2010**, *49*, 7461.
 [16] T. Dvir, M. R. Banghart, B. P. Timko, R. Langer, D. S. Kohane, *Nano Lett.* **2010**, *10*, 250.
 [17] D. D. Young, A. Deiters, *Org. Biomol. Chem.* **2007**, *5*, 999.
 [18] N. C. Fan, F. Y. Cheng, J. A. A. Ho, C. S. Yeh, *Angew. Chem. Int. Ed.* **2012**, *51*, 8806.
 [19] Y. Shamay, L. Adar, G. Ashkenasy, A. David, *Biomaterials* **2011**, *32*, 1377.
 [20] E. S. Lee, K. Na, Y. H. Bae, *Nano Lett.* **2005**, *5*, 325.
 [21] E. S. Lee, Z. Gao, D. Kim, K. Park, I. C. Kwon, Y. H. Bae, *J. Controlled Release* **2008**, *129*, 228.
 [22] C. P. Holmes, *J. Org. Chem.* **1997**, *62*, 2370.
 [23] W. Zhang, Y. A. Shi, Y. Z. Chen, J. A. Ye, X. Y. Sha, X. L. Fang, *Biomaterials* **2011**, *32*, 2894.
 [24] V. Torchilin, *Adv. Drug Deliv. Rev.* **2011**, *63*, 131.
 [25] H. Maeda, G. Y. Bharate, J. Daruwalla, *Eur. J. Pharm. Biopharm.* **2009**, *71*, 409.
 [26] Z. Zhou, B. Chu, V. M. Nace, Y. W. Yang, C. Booth, *Macromolecules* **1996**, *29*, 3663.
 [27] D. Klingler, K. Landfester, *Macromolecules* **2011**, *44*, 9758.
 [28] D. N. Heo, D. H. Yang, H. J. Moon, J. B. Lee, M. S. Bae, S. C. Lee, W. J. Lee, I. C. Sun, I. K. Kwon, *Biomaterials* **2012**, *33*, 856.
 [29] K. Van Butsele, S. Cajot, S. Van Vlierberghe, P. Dubruel, C. Passirani, J. P. Benoit, R. Jérôme, C. Jérôme, *Adv. Funct. Mater.* **2009**, *19*, 1416.
 [30] G. Russell-Jones, K. McTavish, J. McEwan, J. Rice, D. Nowotnik, *J. Inorg. Biochem.* **2004**, *98*, 1625.
 [31] Y. Hu, X. Jiang, Y. Ding, L. Zhang, C. Yang, J. Zhang, J. Chen, Y. Yang, *Biomaterials* **2003**, *24*, 2395.
 [32] N. Rapoport, W. G. Pitt, H. Sun, J. L. Nelson, *J. Controlled Release* **2003**, *91*, 85.
 [33] W. Zhang, Y. Shi, Y. Chen, J. Ye, X. Sha, X. Fang, *Biomaterials* **2011**, *32*, 2894.
 [34] M. Álvarez, A. Best, S. Pradhan-Kadam, K. Koynov, U. Jonas, M. Kreiter, *Adv. Mater.* **2008**, *20*, 4563.
 [35] N. Fomina, C. McFearin, M. Sermsakdi, O. Edigin, A. Almutairi, *J. Am. Chem. Soc.* **2010**, *132*, 9540.
 [36] K. Qi, Q. Ma, E. E. Remsen, C. G. Clark, K. L. Wooley, *J. Am. Chem. Soc.* **2004**, *126*, 6599.